



THE CHIEMGAU METEORITE IMPACT AND TSUNAMI EVENT (SOUTHEAST GERMANY): FIRST OSL DATING

I. Liritzis¹, N. Zacharias², G.S. Polymeris³, G. Kitis⁴, K. Ernstson⁵, D. Sudhaus⁶,
A. Neumair⁷, W. Mayer⁷, M.A. Rappenglück⁷, B. Rappenglück⁷

¹*University of the Aegean, Dept. of Mediterranean Studies, Lab of Archaeometry, Rhodes, Greece*

²*University of the Peloponnese, Dept. of History, Archaeology & Cultural Resources Management,
Laboratory of Archaeometry, 24 100 Kalamata, Greece*

³*R.C. Athena, Cultural and Educational Technology Institute, Archaeometry Laboratory,
Tsimiski 58, GR 67100, Xanthi, Greece*

⁴*Dept of Physics, Aristotle University of Thessaloniki, GR 54124, Thessaloniki, Greece*

⁵*Julius-Maximilians-Universität Würzburg, Am Judengarten 23, 97204 Höchberg, Germany*

⁶*Albert-Ludwigs-Universität Freiburg, Institut für Physische Geographie, 79085 Freiburg, Germany*

⁷*Institute for Interdisciplinary Studies, Bahnhofstrasse 1, 82205 Gilching, Germany*

Received: 01/01/2010

Accepted: 12/06/2010

Corresponding author: liritzis@rhodes.aegean.gr

ABSTRACT

A more exact dating of the Chiemgau meteorite impact in Bavaria, southeast Germany, that produced a large strewn field of more than 80 craters sized between a few meters and several hundred meters, may provide the indispensable fundament for evaluating its cultural implications and thus enable an extraordinary case study. A straightforward answer has not yet been provided due to e.g. scarce existence of diagnostic material, lack of specialised micromorphologists, absence of absolute dating data etc. Here we report on a first OSL dating applied to a catastrophic impact layer that features both impact ejecta and tsunami characteristics attributed to proposed falls of projectiles into Lake Chiemsee in the impact event. The OSL dating was conducted on a quartzite cobble and four sediment samples collected from an excavated archaeological stratigraphy at Lake Chiemsee that comprised also the impact layer.

In a first approach the analyses were based on the assumption of zero luminescence resetting clock from the induced impact shock for the quartzite cobble, and a solar bleaching of tsunami-generated sediments. Optically Stimulated Luminescence (OSL) was applied using the Single Aliquot Regeneration (SAR) protocol and relevant reliability criteria. For sediments the beta-TL method was also applied. Reported ages fall around the beginning of 2nd millennium BC. Special attention is given to the peculiar situation of OSL dating of material that may have been exposed to impact shock of strongly varying intensity, to excavation, ejection and ejecta emplacement, the latter overprinted by and mixed with tsunami transport processes resulting in possibly very complex bleaching scenarios largely differing from the original assumptions.

KEYWORDS: Bavaria, Chiemgau, Luminescence, OSL, Dating, Impact, Meteorite

INTRODUCTION

Here we report on the first OSL dating of a geological record that seems to exhibit a catastrophic layer giving evidence of a meteorite im-

pact-induced tsunami in the roughly 80 km² sized Lake Chiemsee in Bavaria (Germany) (Ernstson et al, 2010) (Fig.1).

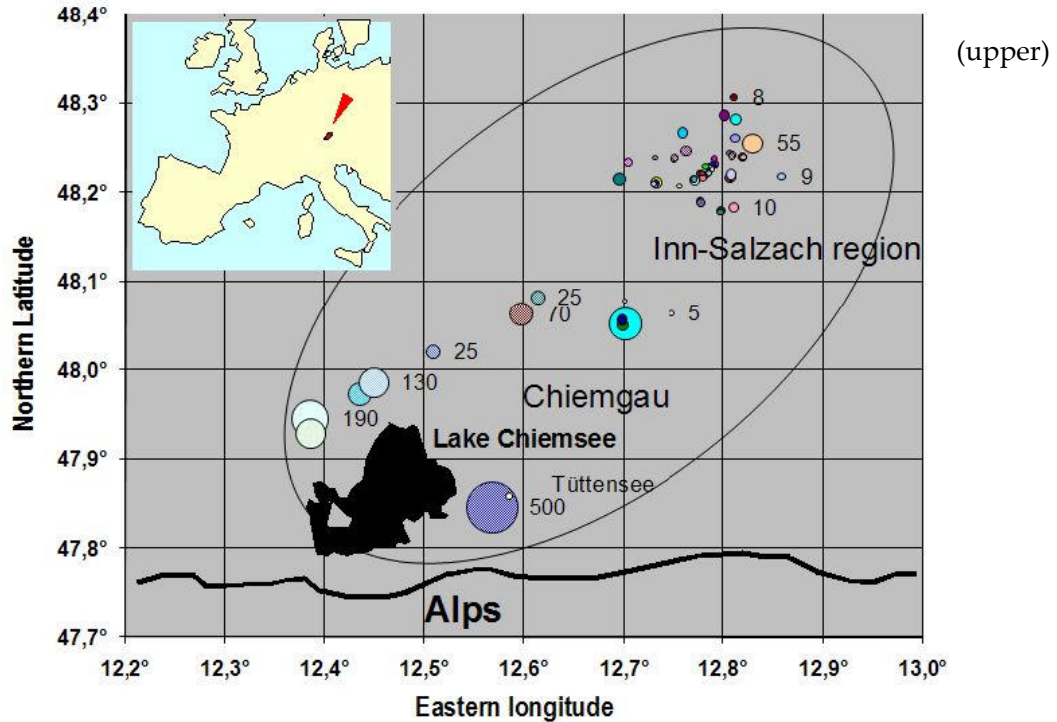
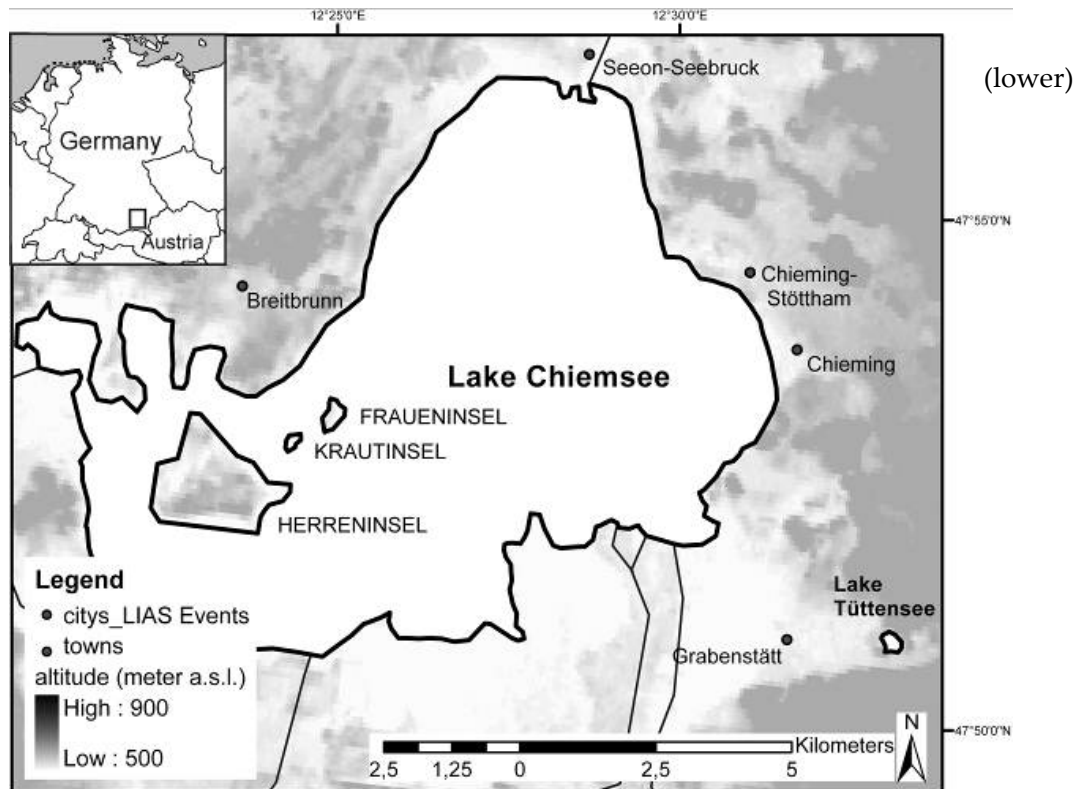


Fig. 1 (Upper) Chiemgau strewn field region showing craters and lakes (not true to scale), and (lower) close up of Chiemsee and Tüttensee lakes environment



An archaeological excavation at Chieming-Stöttham, a location close to the eastern shore of Lake Chiemsee, revealed a remarkable stratigraphy (Neumair et al., 2010): a conspicuous diamictic layer of up to 50 cm thickness is embedded between a layer with very few Neolithic and Bronze Age artefacts (ca. 4400-800 BC) and a layer with a Roman pavement (ca. 2nd century

AD). Geological and mineralogical research provided the evidence that the arguable layer is the relic of a meteorite impact, the so-called Chiemgau impact (Ernstson et al., 2010), and also of a tsunami which had been induced by parts of the meteorite impacting into Lake Chiemsee (Fig. 2)

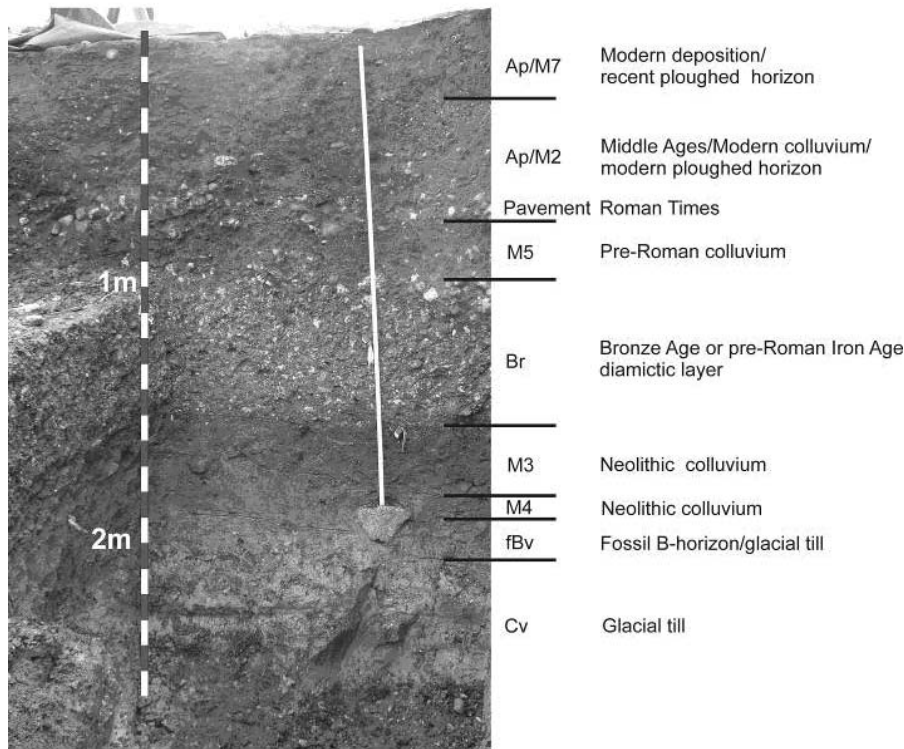


Fig. 2 Excavation trench with stratigraphy

The diamictic layer comprises terrestrial and lacustrine components in a chaotic mixture, shocked clasts and impact spherules, is rich in organic material like wood, charcoal, animal bones and teeth, and contains artefacts. It is strongly heterogeneous and, depending on the location of the layer around Lake Chiemsee, the contribution of the various components differs considerably as does the embedding material.

The Chiemgau impact, causative for the described layer, sticks out among the Holocene meteorite impacts by the fact that the impact is well documented by shock metamorphism of rocks, by the size of the crater strewn field (ca. 1800 km²), the number of craters (ca. 80), the size of the biggest crater (600 m \varnothing) and the variety of secondary effects (Ernstson et al., 2010; Yang et al., 2008), among them the impact-

induced tsunami. The impact catastrophe has been suggested to be reflected in the Greek myth of the fall of Phaethon as a geomyth (Rappenglück and Rappenglück, 2006, Rappenglück et al., 2010), but a good dating of the Chiemgau impact may provide the indispensable fundament for evaluating its cultural implications (Rappenglück et al., 2009).

We deal with five first dates from Optically Stimulated Luminescence (OSL) that may provide clues to dating this impact event and give additional insights into the general possibility of dating tsunami events with reasonable accuracy (Murari et al., 2007) due to pre-depositional zeroing of luminescence by tsunami transport. Thereby, the peculiarity of the interference of impact and tsunami processes is especially addressed.

SAMPLES AND SAMPLE PREPARATION

Material for the OSL dating was taken from the c. 2 m deep excavated section at Chieming-Stöttham that is divided into seven sedimentary units (Fig. 2). It comprised a 3 cm-sized fractured quartzite cobble (sample no. 20, surrounded by soil no. 10) and a sediment sample from the conspicuous diamictic breccia layer, and one sediment sample taken from colluvium beneath and above the diamictite each.

The sandy-clayey matrix of the diamictite similar to the facies of the colluvium above and beneath the diamictite is more or less continuously grading into a breccia of heavily disintegrated clasts interspersed with cobbles and boulders (Neumair et al., 2010). The diamictite is assumed to have originated from a meteorite impact into Lake Chiemsee that produced a doublet crater of about 900 x 400 m size at the lake bottom roughly 1 km apart from the excavation site. On impact and after the shock waves had penetrated the target, both excavation of the water column and of the lake sediments took place according to the generally accepted concept of impact cratering (Melosh, 1989). It is further assumed that ejected water and sediment combined into a big wave running as a tsunami towards the shore thereby probably eroding and incorporating more sediments along the trajectory, before the tsunami discharged its solid carriage onshore.

From thin-section analysis, the quartzite cobble sampled from the diamictite seems to have undergone shock that could have bleached the luminescence palaeodose of the rock (Stankowski, 2007). In a first approximation, the reset is considered complete; discrepancies are subject to the Discussion chapter. Also in a first approximation, the sediment samples are assumed to have been zeroed by sunlight, which will be discussed in more detail below, too.

The setting and stratigraphy are shown in Fig. 2, while the sample positions are compiled in Table 1. Aliquots were prepared with standard procedure. All sediment samples were treated with 10% HCl, followed by two sets of H₂O₂ (5% and 10%) to remove carbonates and organic material, respectively. Wet-sieving using 90-125-250 µm meshes column provided the grain-size distributions of 90-125 and 125-250 µm which favor in OSL quartz dating studies; the later fraction was found in abundance thus all measurements were performed using the 125-250 µm and in only one sample (5-3-M5) use of both fractions was practiced. The next step involved etching in 40% HF to remove the remaining feldspar fraction and the outer layer of quartz grains affected by alpha irradiation and a final wash in 10% HCl to remove any residual soluble fluorides (Zacharias et al., 2009). For quartzite no HF etching was made.

Table 1. Five samples from Chieming-Stöttham and sampling information. Laboratory sample no., excavated profile no., depth and layer (M), gravel fraction, context and expected time (*approx. 60 cm material was already removed before sampling)

Laboratory no.	No. profile, layer / description	Surrounded geometry position	Depth in cm	Gravel faction in %	Expected time, years
RHO-1052	5-3, M5/ brownish black sediment, above diamictite layer	Overlying 15 cm M5, then 5-10 cm Roman pavement; underlying 15 cm M5 followed by 10 cm paving on top of diamictic layer	115	2-5	1300 BC-200 AD
RHO-1051 (dated soil)/ RHO-1050 other soil from same layer	5-4, Br / sediment diamictite layer, sandy loam, brownish black, breccia	Overlying 20 cm Br layer, then M5; underlying 30 cm layer Br	120 (60)*	> 30	2200-300 BC (as RHO-886)
RHO-886	5-2, Sample 20 / quartzite; fractured cobbles from diamictite layer (Br), shock effects	Overlying 20 cm Br, then M5; underlying 30 cm Br	140		2200-300 BC (as RHO-1051)
RHO-1046	5-3, M3 / black sediment, beneath diamictite layer	Overlying 35 cm M3; underlying 7 cm M3 and lower M4	222	1-2	4400-3000 BC, maybe to 800 BC
RHO-1049	5-3, M4 / sediment brownish black	Overlying 25 cm M4 then M3; underlying 20 cm M4, at 10 cm stone 8 cm diam., then 10 cm Bv	263	1-2	4400-3000 BC

INSTRUMENTATION

Dose rates were measured by thick source α -counting with a ZnS detector. The measurements were performed both in the integral and in the pair counting mode, for the discrimination between Th and U. K concentration was determined by SEM-EDX and Flame Atomic Absorption Spectroscopy (FAAS), as well. In cases of lack of FAAS potassium, this was estimated from a linear correlation plot between FAAS and SEM-EDX (Liritzis et al., 2010, in preparation).

All luminescence measurements were performed using the RISØ TL/OSL reader (model TL/OSL – DA – 15), equipped with a high-power blue LED light source, an infrared solid state laser and a 0.075 Gy/s $^{90}\text{Sr}/^{90}\text{Y}$ β -ray source (Bøtter-Jensen et al., 2000). The reader is fitted with a 9635QA PM Tube. All measurements were carried out using a heating rate of 1°C/s, in order to avoid thermal gradient, using a 7.5 mm Hoya U-340 ($\lambda_p \sim 340$ nm, FWHM 80 nm) filter. The power level was software controlled and set at 90% of the maximum power of the blue – LED array, delivering at the sample position ~ 32 mW cm⁻².

Blue stimulation and the single aliquot regeneration (SAR) method was used (300 sec at 125°C), recuperation was corrected and recycling ratios ranged around 1.00±0.10, as evidenced with the preheat test (170-250°C) on natural sample.

METHODS AND FIRST OSL DATING

The age equation used is the standard one:

$$\text{Age} = \text{Equivalent Dose } D_e \text{ (Grays)} / \text{Annual Dose (Grays/year)} \quad (1)$$

The beta-TL/OSL alternative was also applied (Liritzis, 1989) especially at the initial stages of measurements where annual doses were not available, and compared with the detailed eq (1). Age is deduced from a linear log-lin relationship between potassium and beta dose-rate as follows:

$$\log B = 0.244(\pm 4\%) - 0.024 (\pm 3.6\%) \quad (2)$$

and,

$$\text{Age} = 0.0077D / [(B(K-0.35)a + Dc * 10^{-2} * 0.77)], \quad (3)$$

where D=the total equivalent dose D_e , where B from eq (2), K=K₂O%, a=attenuation of betas,

Dc the cosmic ray dose rate (free software is available in: http://www.rhodes.aegean.gr/maa_journal/bTL_onlinetool.html). Whereas dilution exists due to cobbles present the proportional amount is subtracted from potassium values to compensate for the reduced gamma ray dose rate due to K.

Dose Rate Results

Dose rates for rock and sediments were measured employing the alpha counting pairs technique, potassium values with SEM-EDS and FAAS. The water uptake for the area and at a depth of 120-170 cm was taken as 75±25%. Pebbles in the surrounding sediment make up around 2-50% of the sediment volume. The self-gamma of the rock with diameter ~ 3 cm is 16±2% for quartz density (Liritzis, 1987), and beta particle attenuation through grain size (100-150 μm) was 0.89, while cosmic ray dose rate for the area 0.18 mGy/yr (Lake Chiemsee 518 m a.s.l., Prof G. Wagner, Heidelberg, personal commun. to IL, 2009), and an assumed dose of 0.1 mGy/yr for internal quartz radioactivity. Chemical data were transformed to dose rates using the conversion factors of Liritzis and Kokkoris (1992) as applied in Liritzis et al. (2001).

All radioisotopic and age data including some comments are given in Table 2. A worth noting result is the satisfactory concordance between b-OSL and conventional SAR OSL ages.

Equivalent Dose Results

The SAR protocol was applied with the necessary sensitivity etc corrections. Recovered grains made more than a dozen aliquots up to 80 per sample. ED ranged between 7-9.8 Gy for sediments and ~ 3 Gy for the cobble. For the four sediments the doses were in almost accordance to stratigraphic depth ages within the 2nd millennium BC and errors $\sim 10\%$.

The analysis of the date inside the stone (bleached by heating, pressure), refers to the impact which preceded the tsunami event. Thus the soil samples are supposed to have been bleached by sun. The deeper layers could all have the date of the impact or give information

Table 2. Radioisotopic data. Below the U, Th, K entries are the respective surrounding soil data. In parentheses are average data and annual dose rates for respective entries. Equivalent doses from fast component is the net after subtraction of about 6% (NB.: apparent inhomogeneity is noticed on samples from same layer) ^{187}Rb evaluation from $\text{K/Rb}=200/1$; ^{238}U self gamma dose rate was included (Liritzis, 1986); $^{3\beta}\text{-TL/OSL}$ method (Liritzis, 1989), only for sediments. % dilution from cobbles was subtracted from potassium values

Sample no.	Grain size in μm	Water uptake in %	Gamma ray geometry	U in ppm	Th in ppm	K in %	Dose (Gy) / (Annual Dose, in mGy/yr) ¹	OSL age, years B.C./beta-OSL	Archaeological estimation and ^{14}C -age
RHO-1052, sediment, M5	90-125 and 125-250	75±25	Gamma ray geometry	4.84±0.23 (average of 3 soils)	6.35±0.60 (average)	1.77±0.09 or 1.47% K ₂ O (average of 3 soils)	7.07±0.46 (6.44±0.55 deconv. averages of 2 grain sizes) (2.058±0.120)	1130±370 BC (bOSL:1120±300)	ARCH: 1300 BC - 200 AD ^{14}C : 1620-1410 cal. BC, 1435-1215 cal. BC
RHO-1050, sediment, Br/ RHO-1051 dated sample	125-250	75±25		4.02±0.40 (average of 3 soils)	3.65±0.90 (average of 3 soils)	2.13±0.10 =1.77% K ₂ O (average of 3 soils by SEM, FAAS, μXRF), -30% dilution 1.24% K ₂ O	7.75±0.55 or 7.30±0.55 (deconv.) (1.7±20.170)	2250±300 (bOSL:2320±400)	ARCH: 2200-300 BC ^{14}C : 2865-2470 cal. BC
RHO-886, quartzite, sample 20	125-250			0.01±0.001 (soil: 4.06av. of 3.02, 5.60, 3.55)	0.04±0.004 (soil: 3.68av. of 3.55, 4.26, 3.25)	0.001 (1.92 average of soil)	2.71±0.22 (0.68±0.065) ²	1960±400	ARCH: 2200-300BC ^{14}C : 2865-2470 cal. BC
RHO-1046, sediment, M3	125-250	75±25, b-atten.=0.884 (Mejdahl, 1979; Brenan, 2003)	Gamma ray contribution from lower half from M3+M4 calculated to 1/3 rd from M4.	2.84±0.22	8.45±0.77	1.787 (average of layers M3 & M4) = 1.42% K ₂ O	9.74±0.96 (9.35±0.98 from deconv.) / (1.862 +/- 0.127)	3020±400 (bOSL:2680±450) ³	ARCH: 4400-3000 BC, maybe to 800 BC ^{14}C : 2280-1955 cal. BC
RHO-1049, 5-3 M4.	125-250	80 ±20%	Gamma ray evaluated from 27% by volume partial contribution of loam (~1.13%K ₂ O).	4.13±0.22	4.68±0.59	1.50±0.07 (average) = 1.244% K ₂ O	8.67±0.80 (8.15±0.80 deconv.) / (1.62±0.16)	3030±500 (b-OSL: 3460±550)	ARCH: 4400-3000 BC ^{14}C : 2625-2290 cal. BC

about the bleaching by an impact event in dependence to the depth.

The single aliquot regenerative – dose (SAR) protocol, introduced by Murray and Wintle (2000) was used in order to estimate the equivalent dose using blue OSL. The OSL signals were measured for 300 seconds at 125 °C with the intensity held at 90% power, i.e. continuous wave OSL (CW – OSL). The background OSL levels measured after 295-300 seconds exposure were subtracted from the initial luminescence intensity (0-1 seconds) of the decay curves obtained. Each disc was exposed to infrared radiation for 100 seconds at 125 °C before of the laser stimulation, in order to reduce the malign influence of feldspars grain to the signal. The procedure is similar to the double SAR procedure of Banerjee et al. (2001), containing additional SAR steps in order to minimize the need for chemical separation. The post-IR OSL signals resulting from polymineral grains are believed to be dominated by the quartz signal (Roberts and Wintle, 2001; Banerjee et al., 2001).

After the measurement of the natural luminescence signal, each aliquot was given a series of increasing regeneration doses, namely 10, 20 and 40 Gy, in order to obtain a growth curve for each one. The regenerated OSL signal was then measured for three different regeneration doses, including a zero-dose check for the extent of thermal transfer (Aitken, 1998) and a repeat dose point in order to examine the adequacy of the test dose sensitivity-correction procedure. The equivalent dose was then estimated as the dose required producing the natural signal, by interpolating it from the growth curve. The latter was modeled for each aliquot by either a linear or a linear-plus-saturation-exponential growth form.

Prior to each OSL measurement, aliquots should be preheated to remove unstable charge and to equalize charge transfer between natural and laboratory irradiated charge populations (Aitken, 1998). Sensitivity changes induced by preheating, irradiation or optical stimulation were monitored and corrected with the aid of a test dose of 10 Gy, delivered after each regenerative or natural OSL measurement. Before of each test dose measurement, preheat

at 160 °C was applied. The success of the sensitivity test procedure was checked using another measurement cycle, using a regenerative dose set to be equal to the first one. The ratio of the corrected signals, the so-called “recycle ratio” (Murray and Wintle, 2003) indicates the efficiency of the sensitivity correction. The zero dose regenerative cycle is incorporated to measure any reverse charge transfer, known as recuperation, of charge previously photo-transferred to lower temperature traps due to preheating. The mathematical use of recuperation, i.e. the response to 0 Gy dose, is to test whether the growth curve passes from the origin.

SAR protocol enables the estimation of individual equivalent doses for each aliquot. There are several criteria for the acceptance of the equivalent doses of each aliquot. The minimization of the average error of the fitting procedure stands as the most stringent one. Values of equivalent doses lying beyond 3 standard deviations of the mean estimate are omitted. The same happens on the basis of SAR results in a recycle ratio outside the range 1.0 ± 0.1 or in a recuperation-value larger than 20%, when expressed as a fraction of the natural signal.

Although the basic SAR protocol applied to quartz OSL signals is simple, the exact measurement conditions can be varied considerably (Murray and Wintle, 2003). In order to apply the SAR protocol, one has to specify the preheat temperature to be applied. Insufficient preheating may result in erroneous estimations of equivalent doses due to a variety of effects caused to quartz by heating, such as thermal transfer. In order to choose the proper preheat temperature, seven aliquots of the sample (laboratory code 886) were used in order to perform the preheat test (Murray and Wintle, 2003; Polymeris et al., 2009). Seven different preheat temperatures, ranging from 130 to 300 °C, were applied during the SAR procedure, one for each aliquot.

Fig. 3 (a,b) shows the standard four OSL tests applied and the frequency distributions for the D_e estimation, for two sediment samples.

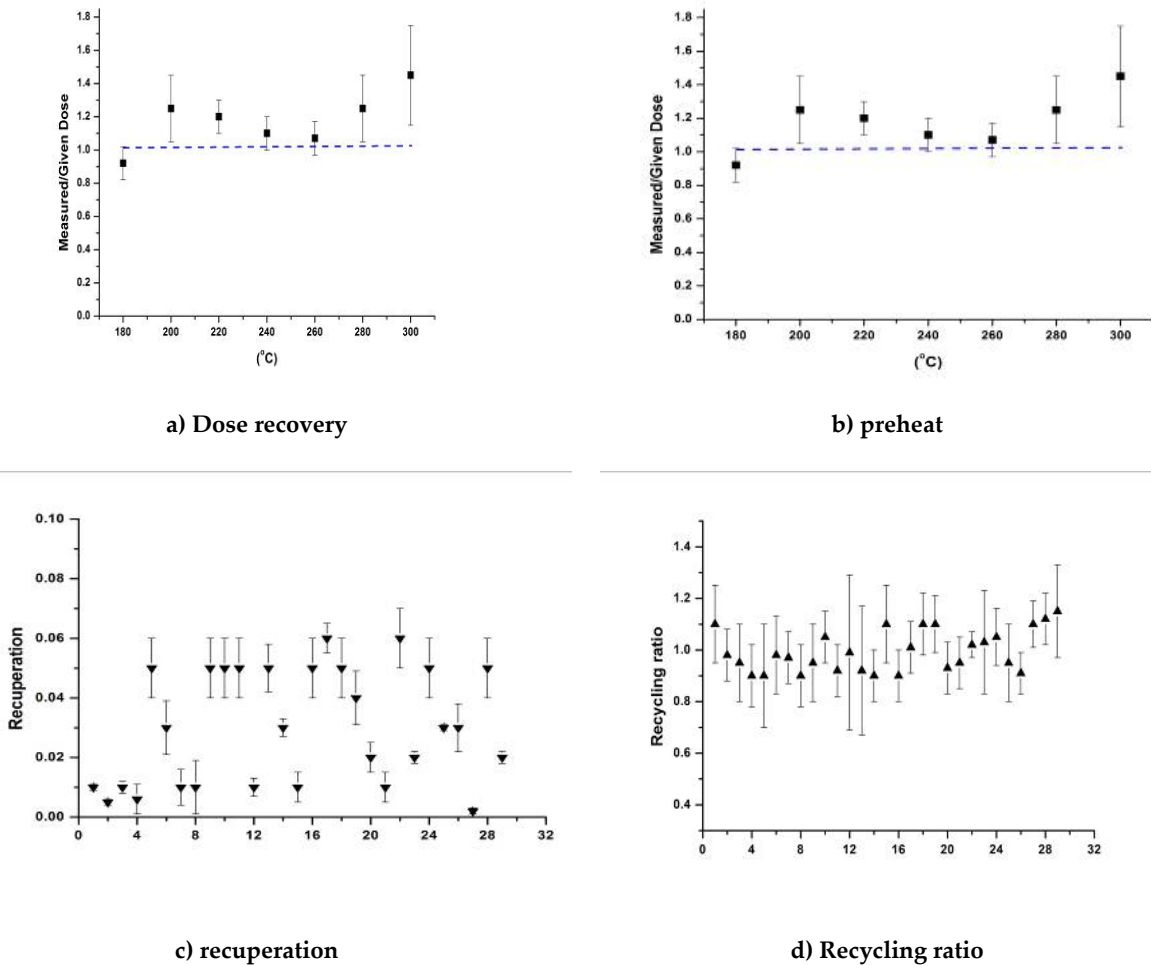


Fig. 3 (a, b, c, d): Four standard OSL tests for sample 5-4 M Br

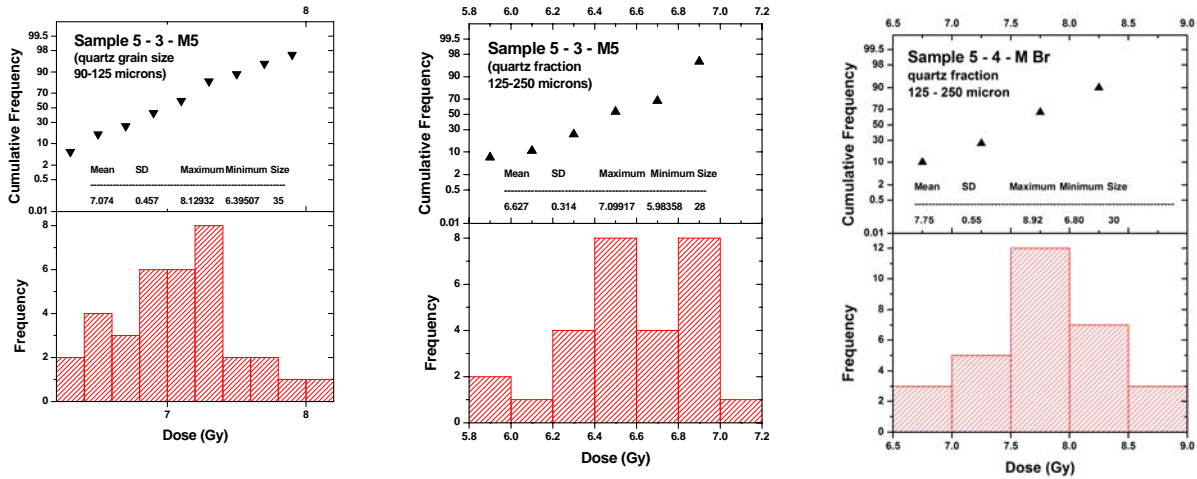
Fig. 5 presents the effect of varying preheat temperatures on the equivalent dose (A), the recycle ratio (B) and the recuperation (C) for the sample 886. The latter is expressed as a percentage on the natural signal. Filled squares represent the individually measured equivalent dose values for each preheat temperature. Equivalent doses are forming a plateau for the preheat temperatures ranging between 170 and 250°C. Similar stability is also observed in the corresponding temperature region for both recycle ratio (being ~ 1.1) as well as the recuperation values (being $\sim 20\%$). However, relatively large recuperation values indicate significant charge transfer due to preheating. Despite the fact of being low, the ED value yielded by the preheat temperature of 170°C is not omitted due to its very close to unity recycle-ratio-value, lowest recuperation value and extremely low dispersions of all three values measured above. Fig. 6

presents an illustrative diagram of the SAR growth curve for the aliquot that was preheated at 170°C.

Earlier work on luminescence properties of glaciofluvial sediments from the same region, the Bavarian Alpine Foreland, demonstrated fast bleaching of quartz signal compared to feldspar with 90% loss within 10s under direct sunlight, while it is zeroed after 1h by bleaching by UV light through a Schott GG 400 filter that cuts short frequency light of the UV lamp and simulates underwater conditions. Moreover, an almost zero signal (remains only 2.6%) is reached within first minute of straight UV illumination, all measurements taken with 0.1 s blue light and IR stimulation. From dose recovery tests based on SAR procedure gave satisfactory results, while TTL is found negligible (Klasen et al., 2006). Although these results apply for the particular grains origin it is interest-

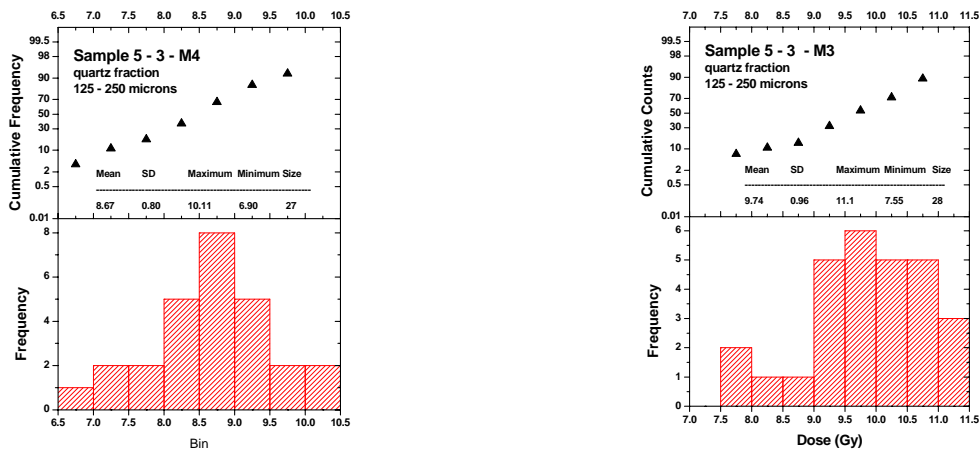
ing to report their luminescence properties compared to present grains from the same region, since we obtained similar properties re-

garding fast bleaching, dose recovery and lack of TTL.



Sample 5 – 3- M5 calculated two different grain fractions

Sample 5 – 4 - M Br



Sample 5 – 3 – M4

Sample 5 – 3 – M3

Fig. 4 Dose distribution and cumulative frequency per number of aliquots used.

Notes: we notice that for all samples the calculated mean values are given in Cumulative Frequencies higher than 50, and especially for the diamictic sample 5-4-Br exceeds 70.

The equivalent dose of the quartzite sample is composed by the mean value (average ED) of these five aliquots (2.71 ± 0.22 Gy) and is indicated by the straight line in panel A of Fig. 5. For the preheat temperature of 150°C there is a substantial increase of both the measured

equivalent dose and especially its dispersions. Finally the temperature of 130°C is omitted mostly because of its extremely large recuperation value (>100%). A summary of the OSL dating data is provided by Table 3.

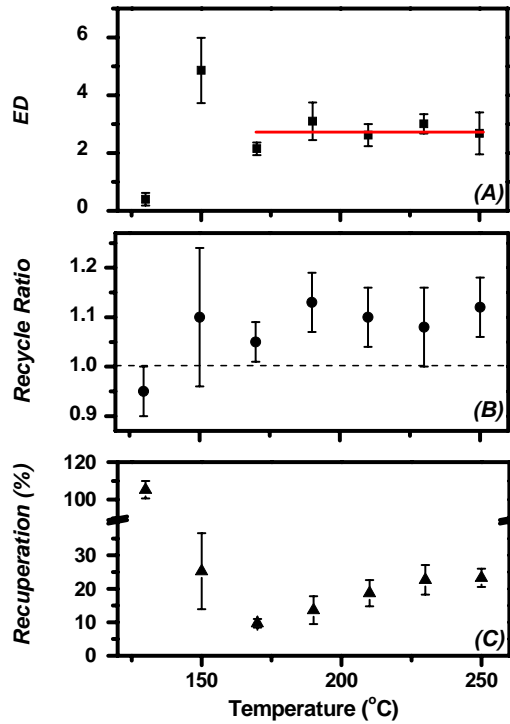


Fig. 5. The dependence of the equivalent dose (A), the recycle ratio (B) and the recuperation (C) on the preheat temperature for the sample RHO-886. Error bars indicate the 1σ deviation. The dashed horizontal line in (B) indicates the optimum value 1 for the recycle ratio. Average ED yielded (2.71 ± 0.22 Gy) is indicated by the straight line in panel A.

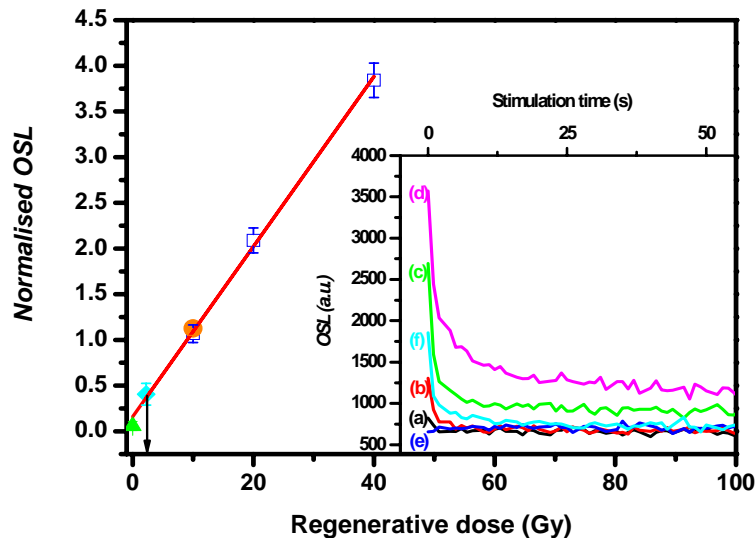


Fig. 6. SAR growth curve, measured for an aliquot from the sample 886, after preheating at 170°C . The ED value is provided by interpolation of the natural normalised OSL signal (filled diamond) onto the growth curve (straight line) resulting from the linear fit to the results of the measurement sequence (open squares). The filled circle represents the recycle point value and the filled triangle the recuperation value. Error bars indicate the 1σ deviation. Inset shows the OSL decay curves for the natural signal (a), the three incremental regenerative doses, i.e., 10, 20 and 40 Gy (b, c and d, respectively) along with the recuperation afterwards (e) and the recycle measurement (f), for the first 55 s of stimulation. The SAR De value yielded (arrow) is 2.15 Gy.

DECONVOLUTION

The checking of fast/slow component in OSL curves was tested by a deconvolution technique. The three components comprising the curves were found by appropriate transformation. In fact the deconvolution can isolate decay components of the OSL signal which occur from incomplete zeroing bleaching and produce erroneous De.

For the deconvolution analysis of the CW-OSL curves, these were transformed into peak-shaped pseudo-LM-OSL (ps-LM-OSL) curves using the transformations introduced by Bulur (2000). In these transformations a new time-dependent variable is defined by the expression

$$u = \sqrt{2 \cdot t \cdot P_{CW}} \quad (4)$$

where u =pseudo time, t = real time, P_{CW} is the total duration of the CW-OSL stimulation. Using this transformation the featureless CW-OSL decay $I(t)$ is transformed into the following peak-shaped ps-LM-OSL intensity $I(u)$:

$$I(u) = u \cdot \frac{I(t)}{P_{CW}} \quad (5)$$

The total time P_{PS-LM} for the transformed ps-LM-OSL curve is obtained from Eq. (6) by setting $t = P_{CW}$ to obtain

$$P_{PS-LM} = \sqrt{2tP_{CW}} = \sqrt{2}P_{CW} \quad (6)$$

For de-convolution purposes the single peak expression of Bulur (2000) were further transformed in order to be a function of the experimental quantities I_m and u_m i.e (Polymeris *et al.*, 2006):

$$I(u) = 1.6487 \cdot I_m \cdot \frac{u}{u_m} \cdot \exp\left[-\frac{u^2}{2u_m^2}\right] \quad (7)$$

The background signal in the case of ps-LM-OSL was simulated by an equation of the form

$$G_{PS}(t) = A_0 + B \cdot \frac{t}{P} \quad (8)$$

where A_0 accounts for the additional background from the dark counts, and B is the average of a zero-dose CW-OSL measurement. P = total measurement time. It is noted that the values of A_0 and B in the background functions are not left to vary arbitrarily during the deconvolution process. Instead, zero dose CW-OSL curves were experimentally obtained and fitted with the background Eq. (8). During the deconvolu-

tion procedure these quantities were left to vary within their evaluated experimental errors. All curve fittings were performed using the MINUIT computer program, while the goodness of fit was tested using the Figure Of Merit (FOM) of Balian and Eddy (1977) given by:

$$FOM = \sum_i \frac{|Y_{Exper} - Y_{Fit}|}{A} \quad (9)$$

where Y_{Exper} is a point on the experimental glow-curve, Y_{Fit} is a point on the fitted glow-curve and A is the area of the fitted curve. The FOM values obtained were between 0.8% and 4% depending upon the statistics.

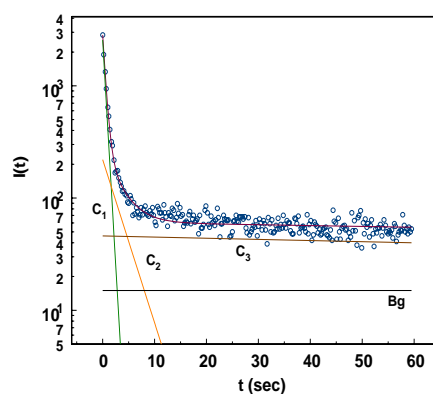
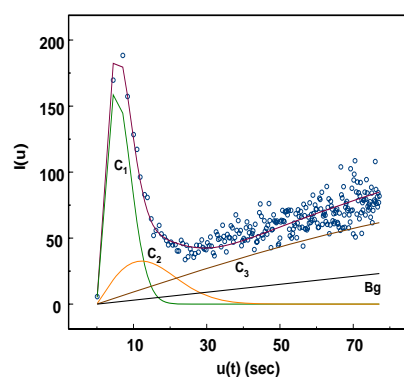


Fig. 7. Deconvolution of the natural OSL (NOSL) signal measured for the M3 sample. Three components were used. Upper panel presents ps-LM-OSL curve, while the lower panel shows the corresponding CW-OSL signal.



Figs. 7, 8 and 9 show the natural OSL curve, as well as the corresponding curves after the regenerative doses of 3 and 9 Gy respectively. In all three cases, upper panels present ps-LM-OSL curves, analysed into three individual OSL components termed as C_1 , C_2 and C_3 , while lower panel figures present the corresponding CW-OSL curves analysed into the same components, after re-transformation of respective ps-LM-OSL curves. Table 3 gives the u_{max} of the pseudo linear modulation OSL from all OSL curves.

Fig. 10 presents an illustrative diagram of the SAR growth curve for a typical aliquot that was collected from sample M3, after using only the C1 integrated OSL signal for calculation analysis. For the 4 different regenerative doses applied, the linearity of the dose response growth curve is prominent. Recycle ratio is very close to unity, while recuperation value is found to be less than 1% of the NOSL C1 signal. Equivalent dose estimation indicated the value of 9.35 Gy, being in great agreement with the conventional SAR analysis value of 9.75 Gy. In all cases, component resolved equivalent dose values were

found to be underestimated by 5-7% compared to the corresponding typical SAR analysis. The reason for this accordance arises from the shape of the CW-OSL signals, exhibiting an extremely rapid decay at the first seconds of stimulation, providing that strong indications about a fast (C1) component being dominant at the initial part of CW-OSL signals. This argument was further supported by the deconvolution analysis as well as Figs 7-9. Nevertheless, the recycling ratio and the recuperation values are much improved by applying the deconvolution procedure.

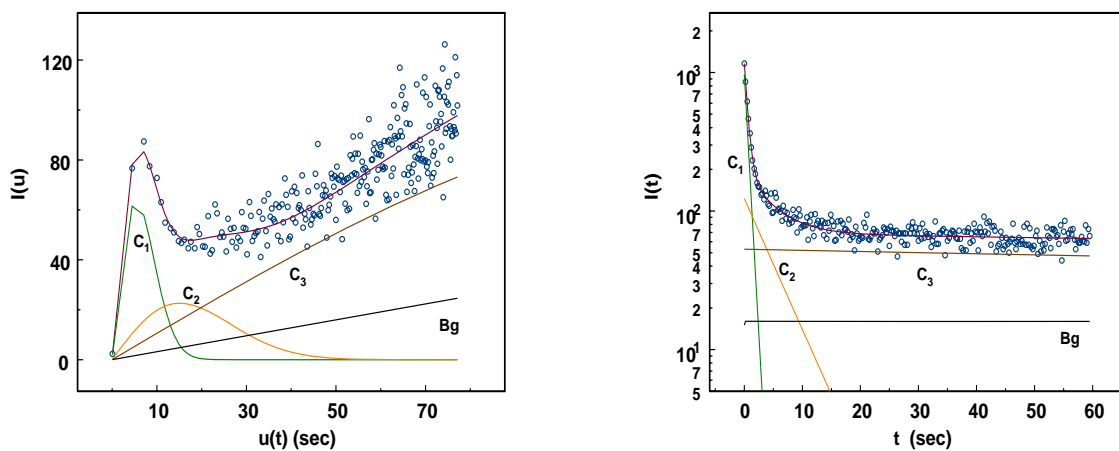


Fig. 8. As in Fig. 7 but for the regenerative dose of 3 Gy. Left panel: ps-LM-OSL curves; Right panel: CW-OSL curves after re-transformation of respective ps-LM-OSL curves.

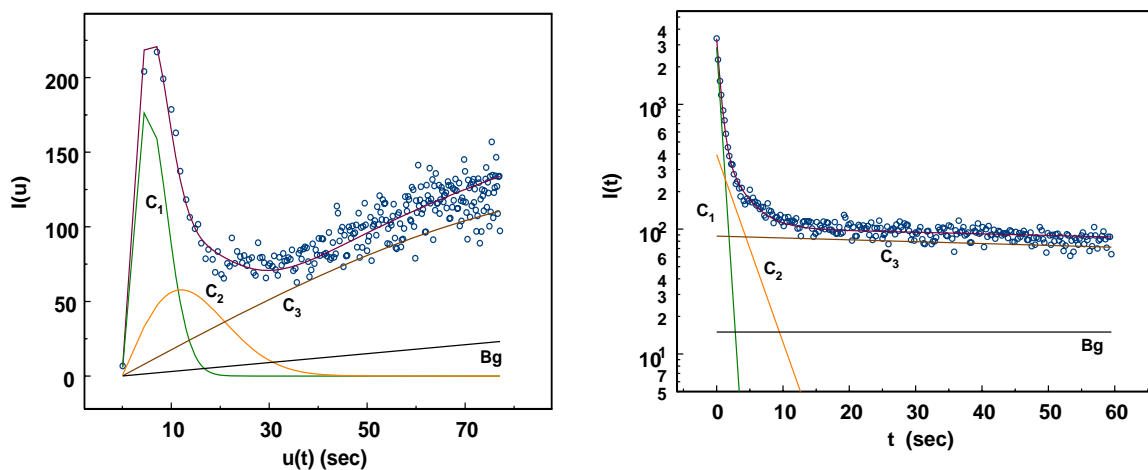


Fig. 9. As in Fig. 7 but for the regenerative dose of 9 Gy. Left panel: ps-LM-OSL curves; Right panel: CW-OSL curves after re-transformation of respective ps-LM-OSL curves.

Table 3. Time maximum of the Pseudo-LM –OSL form all OSL curves.

Component	Pseudo time t_m (sec)	Real time t_m (sec)
C ₁	5.26±0.11	0.27
C ₂	13.13±1.7	1.72
C ₃	143.8±19	206

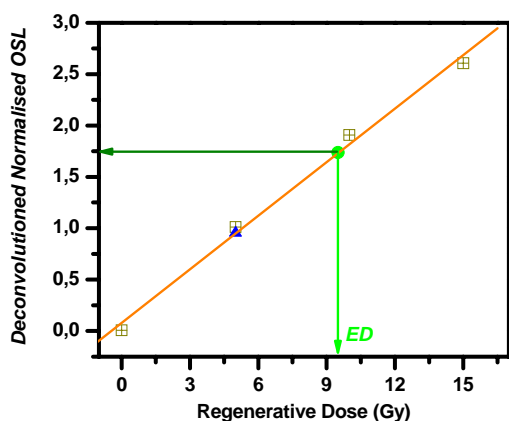


Fig. 10 SAR growth curve, measured for an aliquot from the sample 5-3 M3 after preheating at 240 °C. ED value is provided by interpolation of the natural normalised OSL signal (filled dot) onto the growth curve (straight line) resulting from the linear fit to the results of the measurement sequence (open squares). Filled triangle represents the recycle point value; recuperation value is presented as a square in the axis origin. Error bars indicate the 1 σ deviation. The SAR De value yielded (arrow) is 9.35 Gy.

DISCUSSION

The OSL analyses as described above were based on the preliminary simple assumptions that the impact shock had completely zeroed the quartzite cobble (see, e.g., Stankowski, 2007, Stankowski et al., 2007) and that there was a complete sunlight reset of the sediment samples.

As for the quartzite cobble it is not clear whether the shock (pressure and temperature) was enough for a complete reset. Microscopic isotropic spots seen in thin section could have resulted from local melting of the quartz ensuring temperatures for a zeroing. On the other hand, the melting of quartz requires enormous shock pressures (50 GPa or more) otherwise not documented in the quartzite cobble. Therefore, diaplectic quartz crystals requiring 10-20 GPa

shock pressure only, may alternatively be responsible of the isotropic spots. The related temperatures from shock release are roughly 100-200 °C. While a five minute heating at a temperature of 300 °C virtually removes all the OSL signal of quartz (Smith et al., 1986, 1990), lower temperatures require longer heating to attain the same effect of zeroing. With regard to a presumed shock heating of the quartzite cobble at a temperature probably distinctly lower than 300 °C, a complete reset would have required maybe ten minutes or longer of heating. This seems to have not been the case since shock heating and rapid cooling in the excavation and ejection process must probably have occurred within a fraction of a minute. Therefore it is rather unlikely that the OSL-dated quartzite cobble achieved a zeroing by shock heating, and, hence, the OSL-based age for the diamictic catastrophe layer of 2nd mill BC must rather be considered an age over-estimation. An interesting but yet unanswered question remains whether the pure shock pressure to have possibly produced diaplectic glass in the quartzite cobble could have initiated a resetting, be it completely or partially. For TL dating, pressure in the form of hydrostatic pressure has been suggested to be a possible resetting mechanism (Zöller et al., 2009). The obtained OSL age of 2nd mill BC is speaking in favour of an at least partial reset by the impact.

For the sediment sample taken from the diamictic impact layer, the validity of the assumed zeroing by sunlight may likewise be discussed. Different from dating a "normal" tsunami with a proposed pre-depositional zeroing of luminescence by transport (Murari et al., 2007), the impact-induced tsunami under consideration involves additional aspects since both impact and tsunami transport bleaching apply in the case of the Chiemgau impact.

In view of the impact-related OSL dates we have to consider that pressures and temperatures shock waves produced in the impact event decrease with depth. Therefore, during the impact the grains in older strata should be bleached to different degrees, i.e., from complete bleaching to partial or no bleaching at all (Stankowski et al., 2007).

While the model of Stankowski et al. (2007) addresses an important point, the practice of impact physics shows that additional, more complex aspects must be taken into account. The decrease of pressure and temperature with depth in the contact and compression stage of impact cratering may apply on the whole, but shock propagation in inhomogeneous media like rocks is extremely intricate depending on lots of parameters like density, porosity, water content, rock boundaries etc. Consequently, complex interference processes shock waves normally undergo, may lead to shock effects of drastic intensity fluctuations even within small volumes. Therefore, shock magnitudes depending on depth in autochthonous rocks can only statistically be quoted and not in selected samples. Even in one individual sample, shock levels may vary by orders of magnitude.

In the case of OSL dating of impact ejecta matters may be even more complicate. While the crater is being excavated, peculiarities of impact physics, namely the special trajectories of the impact ejecta, have the result that rock material starting from far-off depths may be emplaced side by side in the ejecta deposit. Due to this process, it is not at all a surprise that Stankowski et al. (2007) observed remarkably varying bleaching effects in quartz of impact-affected samples.

Confusion even increases in the case of impact ejecta produced by impact into a lake and integrated in a tsunami transport. In this case sunlight could also have contributed to bleaching. The Stöttham diamictite, from which the OSL dating samples treated here have been gathered, had probably been subject of such a complex process.

Of course, provided all shocked and unshocked excavated ejecta were exposed to sunlight along the tsunami trajectory, the preliminary assumption of complete reset would have been fulfilled. Apart from the question whether there was any sunlight or even daylight at all in and shortly after the extensive impact event, the proposed mixed ejecta/tsunami transport could have hampered a complete exposure of the material finally deposited as the Stöttham diamictite. The observation of abundant strongly fractured however coherent cob-

bles and boulders within the diamictic sediment (Neumair et al., 2010) points to confining pressure that was maintained along the tsunami trajectory at least within parts of the material. Consequently, the sediment sample may have consisted of particles of strongly varying shock load and also of strongly varying sunlight or daylight exposure, respectively. Hence, a complete resetting of the sediment sample remains questionable, and the obtained preliminary OSL age may represent again an age over-estimation.

The OSL ages (mid 2nd mill BC to end of 3rd mill BC) of the sediment samples taken from beneath and above the impact layer may also be discussed. While the OSL age of the sample from beneath the diamictite may reasonably reflect the luminescence zeroing in the time of the Bronze Age, the OSL dating of the colluvium covering the impact diamictite carries more uncertainties. It cannot be excluded that at least the basal part of the colluvium represents reworked ejecta/tsunami material that was deposited immediately after the emplacement of the diamictite posing similar questions about a complete or only partial reset.

An interesting aspect of OSL dating of impacts and impact-induced tsunamis has as far as we know not been considered at all. Energetic neutron bombardment suggested for impact events (Brown and Hughes, 1977) must lead to strongly enhanced gamma radiation in the impact area. Neutron collisions with hydrogen nuclei especially in hydrogen-rich matter (water!) involve a slow-down to so-called thermal neutrons which may be captured by chlorine, silicon and other nuclei leading to the emission of a highly energetic gamma radiation. The effect on quartz and feldspar used in OSL dating may be considerable but has obviously not been studied hitherto.

CONCLUSION

The study as presented here focuses on a new aspect of OSL dating. While OSL datings of both impacts and tsunamis have been considered and performed on their own, we address OSL dating of a meteorite impact, the Chiemgau impact event, combined with a tsunami induced by that impact.

The most pertinent OSL ages are related to a catastrophic impact layer that is assumed to have originated from a combination of impact ejecta and tsunami transport and that has also been radiocarbon-dated and dated by archaeological objects. The artefacts comprise Neolithic to the Urnfield culture (4400-800 BC) (Möslein, 2009). One potsherd and an iron lump attribute to the Hallstatt era (800-475 BC). A higher age is given by a ^{14}C -analysed charcoal sample, but reworking of the carbon material is a fundamental problem in this case.

The corresponding OSL ages as presented here are roughly compatible with the mentioned Neolithic to Urnfield culture artifacts and in the case of a complete resetting of the OSL clock could place the impact to the Bronze Age. A larger discrepancy in age is found considering the find of the Hallstatt potsherd and the iron lump within the diamictite. With regard to the peculiar effects the impact may have introduced to the OSL reset, this is not so much surprising and corresponds with an incomplete zeroing leading to a general age over-estimation.

Therefore, at the moment the OSL dating of the Chieming-Stöttham site provides very

probably a maximum age for the Chiemgau impact at least and, hence, helps to set limits to the archaeological dating of the event. In further progress it perhaps gives a basis for considering the cultural consequences of the Chiemgau impact. At the same time, the mere fact of a (partial) resetting within the quartzite cobble gives additional clear evidence of the Chiemgau impact event provided normal processes like exposure to fire or other resetting mechanisms having acted through and though can be excluded.

We further conclude that establishing and dating an impact by the OSL method, as earlier suggested by Stankowski (2007) and Stankowski et al. (2007), has to consider the shock intensities documented in the matter to be analysed, thus warranting a complete zeroing or pointing to a partial reset only, respectively. Based on a systematic investigation of shock-dependent OSL resetting mechanisms, and understanding the effects neutron and associated strong gamma radiation may impinge, OSL dating of impacts may become an interesting tool in impact research, last but not least in the case of studying an impact-induced tsunami.

ACKNOWLEDGEMENTS

We thank the CETI lab of archaeometry for some measurements and Prof C. Sideris for mineralogical observations.

REFERENCES

- Aitken, M.J. (1998). *An Introduction to Optical Dating*. Oxford University Press, Oxford.
- Bøtter-Jensen, L., Bulur, E., Duller, G.A.T., Murray, A.S. (2000). Advances in luminescence instrument systems. *Radiation Measurements* 32, 523–528.
- Banerjee, D., Murray, A.S., Bøtter-Jensen, L., Lang, A. (2001). Equivalent dose estimation using a single aliquot of polymineral fine grains. *Radiation Measurements* 33, 73–94.
- Balian, H.M. and Eddy, N.W. (1977). Figure-of-merit (FOM): An improved criterion over the normalized Chi-squared test for assessing goodness-of-fit of gamma-ray spectral peaks. *Nuclear Instruments and Methods* 145: 389–395, DOI 10.1016/0029-554X(77)90437-2.
- Brennan, B.J (2003). Beta doses to spherical grains. *Radiation Measurements*. 37, 299-303.
- Brown, J.C., Hughes, D.W. (1977). Tunguska's comet and non-thermal C^{14} production in the atmosphere. *Nature* 268, 512-514.
- Bulur, E., Bøtter-Jensen, L., Murray A.S. (2000). Optically stimulated luminescence from quartz measured using the linear modulation technique. *Radiation Measurements* 32: 407–411.
- Ernstson, K., Mayer, W., Neumair, A., Rappenglück, B., Rappenglück, M.A., Sudhaus, D., Zeller, K.W. (2010). The Chiemgau Crater Strewn Field: Evidence of a Holocene large impact event in Southeast Bavaria, Germany. *Journal of Siberian Federal University. Engineering & Technologies* 1, 72-103.

- Klasen, N., Fiebig, M., Preusser, F. and Radtke, U. (2006). Luminescence properties of glaciofluvial sediments from the Bavarian Alpine Foreland. *Radiation Measurements*, 41, 866-870.
- Liritzis, I. (1986). The significance of gamma- self- dose and β -ranges in ceramics revisited. *Revue d'Archeometrie*, 10, 95-102.
- Liritzis, I. (1989). Dating of quaternary sediments by beta thermoluminescence: investigations of a new method. *Annales Soc. Geolog. Belgique*, T.112, 1, 197-206.
- Liritzis, I. and Kokkoris, M. (1992). Revised dose-rate data for thermoluminescence / ESR dating. *Nuclear Geophysics* 281, 6 (3), 405-411.
- Liritzis, I., Galloway, R.B, Katsonopoulou, D. and Soters, D. (2001). In search of ancient Helike, Gulf of Corinth, Greece. *Journal of Coastal Research*, 17, 1, 118-123.
- Liritzis, I., Zacharias, N., Sakalis, A., Tsirliganis, N., Polymeris, G.S. (2010). Potassium determination from SEM, FAAS, and XRF: some notes. *Medit. Archaeol. & Archaeometry* (in press).
- Melosh, H.J. (1989). *Impact cratering. A geologic process*. Oxford Univ. Press, Oxford.
- Mejdahl, V (1979). Thermoluminescence dating: beta dose attenuation in quartz grains. *Archaeometry* 21, 1, 61-72.
- Möslein, S. (2009). Grabungsbericht. Chieming TS, Stöttham-Dorfäcker 2007/08. Bad-Tölz, unpubl.
- Murari, M.K., Achyuthan, H., Singhvi, A.K. (2007). Luminescence studies on the sediments laid down by the December 2004 tsunami event: Prospects for the dating of palaeo tsunamis and for the estimation of sediment fluxes. *Current Science* 92, 367-371.
- Murray A.S., Wintle, A.G. (2000). Luminescence dating of quartz using an improved single – aliquot regenerative – dose protocol. *Radiation Measurements* 32, 57 – 73.
- Murray, A.S., Wintle, A.G. (2003). The single aliquot regenerative dose protocol: potentials for improvements in reliability. *Radiation Measurements* 37, 377 – 381.
- Neumair, A., Ernstson, K., Mayer, W., Rappenglück, B., Rappenglück, M.A., Sudhaus, D. (2010). Characteristics of a Holocene impact layer in an archeological site in SE-Bavaria, http://impact-structures.com/news/Stoettham_c.pdf (accessed 26/06/2010).
- Polymeris, G.S., Tsirliganis, N.C., Loukou Z. and Kitis G. (2006). A comparative study of anomalous fading effects of TL and OSL signals of Durango apatite. *Physica Status Solidi A* 203(3): 578 – 590.
- Polymeris, G.S., Kitis, G., Liolios, A.K., Sakalis, A., Zioutas, K., Anassontzis, E.G., Tsirliganis, N.C. (2009). Luminescence dating of the top of a deep water core from the NESTOR site near the Hellenic Trench, east Mediterranean Sea. *Quaternary Geochronology*, 4, 68 – 81.
- Rappenglück, B., Rappenglück, M. (2006). Does the myth of Phaethon reflect an impact? Revising the fall of Phaethon and considering a possible relation to the Chiemgau Impact. *Mediterranean Archaeology & Archaeometry*, Spec. Issue 6, 101-109.
- Rappenglück, B., Ernstson, K., Mayer, W., Neumair, A., Rappenglück, M.A., Sudhaus D., Zeller, K.W. (2009). The Chiemgau impact: An extraordinary case study for the question of Holocene meteorite impacts and their cultural implications. *Cosmology Across Cultures ASP*, Conference Series 409, 338-343.
- Rappenglück, B., Rappenglück, M.A., Ernstson, K., Mayer, W., Neumair, A., Sudhaus D., Liritzis, I. (2010). The fall of Phaethon: a Greco-Roman geomyth preserves the memory of a meteorite impact event in Bavaria (Southeast Germany), *Antiquity* 84, 428-439.
- Roberts, H.M., Wintle, A.G. (2001). Equivalent dose determinations for polymineralic fine-grains using the SAR protocol: application to a Holocene sequence of the Chinese Loess Plateau. *Quaternary Science Reviews* 20, 859 – 863.
- Smith, B.W., Aitken, M.J., Rhodes, E.J., Robinson, P.D., Geldard, D.M. (1986). Optical dating: Methodological aspects. *Radiation Protection Dosimetry* 17, 229–233.
- Smith, B.W., Rhodes, E.J., Stokes, S., Spooner, N.A. (1990). The optical dating of sediments using quartz. *Radiation Protection Dosimetry* 34(1), 75–78.

- Stankowski, W.T.J. (2007). Luminescence dating as a diagnostic criterion for the recognition of Quaternary impact craters. *Planetary and Space Science* 55, 871-875.
- Stankowski, W.T.J. Raukas, A., Bluszcz, A., Fedorowicz A. (2007). Luminescence dating of the Morasko (Poland), Kaali, Ilumetsa and Tsõõrikmäe (Estonia) meteorite craters. *Geochronometria* 28, 25-29.
- Yang, Z.Q., Verbeek, J., Schryvers, D., Tarcea, N., Popp, J., Rösler, W. (2008). TEM and Raman characterisation of diamond micro- and nanostructures in carbon spherules from upper soils. *Diamond and Related Materials*, 17, 937-943.
- Zacharias, N., Bassiakos, Y., Hayden, B., Theodorakopoulou, K., Michael, C.T. (2009). Luminescence dating of deltaic deposits from eastern Crete, Greece: Geoarchaeological implications, *Geomorphology* 109, 46-53.
- Zöller, L., Blanchard, H., McCammon, C. (2009). Can temperature assisted hydrostatic pressure reset the ambient TL of rocks? - A note on the TL of partially heated country rock from volcanic eruptions. *Ancient TL*, 27 (1), 15-22.